Modelling fuel consumption and pollutant emissions based on real-world driving patterns: the HBEFA approach

Peter de Haan*

Swiss Federal Institute of Technology,
Department of Environmental Sciences,
ETH Zentrum HAD, 8092 Zurich, Switzerland
E-mail: dehaan@env.ethz.ch
*Corresponding author

Mario Keller

INFRAS, Muehlemattstr 45, 3007 Bern, Switzerland
E-mail: bern@infras.ch

Abstract: Emissions of passenger cars and light-duty vehicles with complex exhaust gas after-treatment are difficult to predict, especially if the prediction is only based on kinematic parameters without vehicle-specific data. A new method for modelling fleet emission factors based on testbench data is presented. It has been used for modern passenger cars and light-duty vehicles (EURO-2 and -3) in the new version 2.1 of the German-Austrian-Swiss Handbook Emission Factors for Road Transport (HBEFA). The new method, not relying on vehicle-specific data, avoids decomposing the measured real-world driving behaviour and all associated uncertainties. Emission factors can be predicted for any given driving pattern which is characterised through kinematic parameters or representative time series of vehicle speed. The methodology determines the linear combination of measured driving patterns that is most representative for the driving pattern whose emissions are to be predicted. The approach is illustrated using testbench real-world measurements of 44 passenger cars of technology stages EURO-2 and -3.

Keywords: emission modelling; emission factors; road transport; testbench measurements; driving cycles; real-world emissions; instantaneous modelling.

Reference to this paper should be made as follows: de Haan, P. and Keller, M. (2004) 'Modelling fuel consumption and pollutant emissions based on real-world driving patterns: the HBEFA approach', *Int. J. Environment and Pollution*, Vol. 22, No. 3, pp.240–258.

Biographical notes: Peter de Haan studied physics at Swiss Federal Institute of Technology (ETH) and obtained his doctoral degree on air quality modelling. From 1998 to September 2003, he worked as a Research Associate at INFRAS in Bern, Switzerland, modelling atmospheric emissions from transport, especially road transport, and modelling air quality. Since October 2003, he is Senior Research Associate at the Institute for Human-Environment Systems at ETH in Zurich.

Mario Keller received his master degree as a traffic engineer from ETH in Zurich, and a master degree in transportation science from MIT. He joined INFRAS in 1983, and is a partner and member of the board of directors since 1991. He specialises on road transport emission modelling, traffic modelling, and related consulting services.

1 Introduction

Atmospheric pollutants cause human health problems (Dab et al., 2001; Hoek et al., 2000), and therefore are of major concern. Since the 1980s, emissions and air pollution levels of nitrogen oxides (NO_x), carbon monoxide (CO) and volatile organic compounds (VOC) have become legislated, monitored, and modelled. In more recent years, fine particulate matter (PM) has become the prime focus. Recent epidemiological studies have found statistically significant relationships between particulate air pollution and human health effects; for a good review, see Pope et al. (1995). Road transport belongs to the major sources of personal exposure to atmospheric pollutants for all criteria pollutants, CO, NO_x, PM, and VOC (Skov et al., 2001; Janssen et al., 2001; Vardoulakis et al., 2002; Chang, 2002; Sapkota and Buckley, 2003; Kunzli et al., 2000; Fischer et al., 2000). Since human receptors are often very close to these emission sources, road emissions contribute to personal exposure even more than would be expected from their share on total emissions. Emissions from road transport also are of high importance in urban environments, where emission factors are above-average and dispersion conditions are less efficient than in rural areas (de Haan et al., 2001).

Exhaust gas after-treatment systems have been introduced since the mid-1980s, together with, and driven by, legislation enforcing emission limits that were lowered several times both in North America and Europe. The resulting reduction of (absolute) overall emission levels has been accompanied by an increase in the (relative) spread of individual emission levels. Vehicles now differ much more from each other than some twenty years ago. As a direct consequence, this increased complexity of exhaust gas after-treatment systems leads to a corresponding decrease in prediction power of the emission factor modelling approaches.

To illustrate this, Table 1 shows the NO_x emission functions for passenger cars, as used in the COPERT3 road emission model (Ntziachristos and Samaras, 2000). COPERT3 is an emission model using linear regression on emission results from complete driving cycles (without decomposition into driving patterns or into second-by-second instantaneous data), and uses average trip speed as sole explaining variable. Taking the Pearson coefficient (R^2 values in Table 1) as measure for the prediction power of the emission functions, a drastic decrease from pre-ECE vehicles (where vehicle emission were high and showed good correlation with average speed) to Euro-1 vehicles (with generally low emissions, but with large differences between vehicles and operating conditions, and no dependence anymore on the average speed) is observed. For Euro-1 vehicles, R^2 drops down to values between 0.12 and 0.01, depending on engine capacity class. Note that in COPERT3, all emission factors for Euro-2, Euro-3 and Euro-4 vehicles are derived from the Euro-1 emission function using reduction factors.

Table 1 NO_x emission factor functions of COPERT3 (Ntziachristos and Samaras, 2000). V denotes average driving cycle speed in km/h

Vehicle class	*Engine capacity* [l]	*NO_x emission factor* [g/km]	*R2* [–]
pre-ECE & ECE 15-00/01	<1.4	$1.173 + 0.0225V - 0.00014V^2$	0.92
	1.4–2.0	$1.360 + 0.0217V - 0.00004V^2$	0.96
	>2.0	$1.5 + 0.03V + 0.0001V^2$	0.97
ECE 15-02	<1.4	$1.479 - 0.0037V + 0.00018V^2$	0.71
	1.4–2.0	$1.663 - 0.0038V + 0.00020V^2$	0.84
	>2.0	$1.87 - 0.0039V + 0.00022V^2$	0.82
ECE 15-03	<1.4	$1.616 - 0.0084V + 0.00025V^2$	0.84
	1.4–2.0	1.29e0.0099V	0.80
	>2.0	$2.784 - 0.0112V + 0.000294V^2$	0.58
ECE 15-04	<1.4	$1.432 + 0.003V + 0.000097V^2$	0.67
	1.4–2.0	$1.484 + 0.013V + 0.000074V^2$	0.72
	>2.0	$2.427 - 0.014V + 0.000266V^2$	0.80
Improved conventional	<1.4	$- 0.926 + 0.719\ln(V)$	0.88
	1.4–2.0	$1.387 + 0.0014V + 0.000247V^2$	0.88
Open loop	<1.4	$- 0.921 + 0.616\ln(V)$	0.79
	1.4–2.0	$- 0.761 + 0.515\ln(V)$	0.50
EURO I	<1.4	$0.5595 - 0.01047V + 10.8E\text{-}05V^2$	0.12
	1.4–2.0	$0.526 - 0.0085V + 8.54E\text{-}05V^2$	0.08
	>2.0	$1.360 + 0.0217V - 0.00004V^2$	0.01

First-generation so-called instantaneous emission modelling did not use car-specific variables (de Haan and Keller, 2000), but encountered important limitations (Sturm et al., 2000). The increased car-to-car variance of emission behaviour has contributed to a certain bifurcation in the research on road transport emissions. On the one hand, current research on instantaneous emission modelling is moving towards sub-models tailored to each vehicle individually, measuring with 10 Hz resolution, and employing dynamical instead of static corrections for transport time in the exhaust system. On the other hand, fleet emission factor modelling cannot benefit from these recent advances in instantaneous emission modelling.

If fleet emission factors would be constructed out of a weighted sample of vehicle-specific emission forecasts, different sets of weighting factors have to be established for each reference year, for each street category, and for each country. Only little is known on future carmaker's strategies in emission reduction and exhaust gas after-treatment, so such weighting factors cannot be estimated for future reference years. This counteracts any gain in statistical performance due to the inclusion of vehicle-specific information.

For the new version 2.1 of the official German–Austrian–Swiss Handbook Emission Factors Road Transport (HBEFA), it has therefore been decided to discontinue the previously used instantaneous modelling approach. Instead, a new method has been developed where emission forecasting is done based on linear combinations of measured driving patterns, which are not being decomposed.

The topics of the present paper are the modelling method based on linear combinations of driving patterns (Section 2), the set of real-world driving cycles especially developed for emission factor modelling (Section 3), and an exemplary forecast of three non-measured driving patterns as an illustration of the presented method (Section 4). To validate the new approach, we use measurements for 12 driving patterns from 44 gasoline and diesel passenger cars conforming to Euro-2 and Euro-3 legislation (Section 5), and perform a cross-validation where each of the 12 driving patterns is being forecasted by the remaining 11 (Section 6). Finally, we discuss the advantages and disadvantages of the new method (Section 7).

2 Modelling approach

Whereas an instantaneous emission model had been used for the original version 1.1 of the German–Austrian–Swiss Handbook Emission Factors for Road Transport (HBEFA) (INFRAS, 1995; Keller and de Haan, 1999), a new modelling approach has been developed for application to emission data from passenger cars and light-duty vehicles complying to Euro-2 or Euro-3 emission standards. The original approach had a second-by-second approach and binned data into cells according to speed and the product of speed and acceleration. It neglected the temporal autocorrelation of emission behaviour; emission data from many different vehicles was binned into one matrix. Data in each of the matrix cells often exhibited very large standard deviations.

The new method, presented in this section, is designed to be used in the modelling of emission factors, where emission factors are not expressed as a continuous function (of average speed and/or other parameters), but are parameterised as a discrete function of so-called traffic situations. Such traffic situations are characterised by a speed profile. Such a speed profile is hereafter called ‘driving pattern’. The driving pattern enables to compute a wide range of kinematic parameters for any traffic situation, so that a quantitative description of the traffic situation is available.

For such a traffic-situation-oriented modelling approach, the method is as follows:

- testbench measurements are available from (sub-)cycles (hereafter called ‘source’ [sub-]cycles)
- through their speed profile, kinematic parameters of these ‘source’ (sub-) cycles are computed
- for the traffic situations for which emissions factors finally are needed, representative speed profiles must be supplied
- from these speed profiles (called ‘target’ driving patterns hereafter), kinematic parameters are computed
- the optimal linear combination of ‘source’ (sub-)cycles for each of the ‘target’ driving patterns is determined, where ‘optimal’ means that the sum of squared differences (between ‘target’ and linear combination of ‘sources’) for a user-specified set of kinematic parameters is minimal.

3 Real-world testbench driving cycles

Within the framework of version 1.1 of HBEFA (Keller et al., 1995), an extensive measurement campaign on real-world driving behaviour has been conducted on Swiss roads. A classification scheme was set up to characterise

- road categories (highway, extra-urban, urban)
- road environmental characteristics (number of driving lanes, road gradient, speed limitation, whether the road was straight or curved, etc.).

The measurement campaign was conducted with cars equipped with speed and time logging devices. The cars were driven by special drivers, who were instructed to follow the traffic flow. In the case of very low traffic, the drivers were told to drive freely, obeying the speed limits.

The campaign recorded 759,299 s of driving behaviour, along with parameters characterising the road. To obtain characteristic driving patterns, a statistical cluster analysis was performed. For this, the driving recordings were cut into driving patterns according to changes in road characteristics. Each driving pattern had 14 parameters describing the type of the road (average travel speed, sign of the change of the average speed during the driving pattern, standard deviation of speed, road gradient, percentage of time with speed zero, percentage of time with constant driving speed, length of the driving pattern, amount of traffic in veh/hour, etc.). The cluster analysis was conducted separately for highways on the one hand and for extra-urban and urban driving on the other. Extra-urban and inner-urban driving was treated together because there is no clear boundary between the two. A total of 32 clusters were identified.

These original on-road recordings of driving behaviour have recently been reprocessed. The so-called 'Handbook real-world driving cycles' were developed in 1999 (Stahel et al., 2000). These cycles now are being used regularly at EMPA (Swiss Federal Laboratories for Materials Testing and Research) in Switzerland for every passenger car and light-duty vehicle being tested within the framework of the national emission factor study. They have been derived with the goal to bring directly onto the testbench on-road recordings of real-world driving, in order to be able to measure real-world emissions which are truly representative (de Haan and Keller, 2000). More details on which criteria have been applied to select those 'driving patterns' being representative for the whole cluster of on-road recordings can be found in de Haan and Keller (2001). The selected raw on-road recordings were smoothed with a running-mean smoother in order to obtain driving cycles suitable for testbench measurements.

The 12 most important (with respect to vehicle performance, i.e., annual mileage) driving patterns have been selected to be represented in the new set of real-world testbench driving cycles directly. Each driving cycle consists of three driving patterns. Their speed time series (also called speed curves) are depicted in Figure 1. Complementing the speed time series, we also use the $(v, v \cdot a)$ -matrix, which is given in Figure 2 for each driving pattern. The $(v, v \cdot a)$-matrix is computed by binning each second of the speed time series according to the speed, v, and the product of v and the instantaneous acceleration, a. Cell boundaries of the matrix are 10 km h^{-1}, 20 km h^{-1}, 30 km h^{-1}, etc., for v, and ± 2.5 m^2 s^{-3}, ± 7.5 m^2 s^{-3}, and ± 12.5 m^2 s^{-3} for $v\,a$. Cells are indicated using the mean values of v and $v\,a$ they contain, e.g., the matrix cell (35 km h^{-1}, + 5 m^2 s^{-3}) holds all second-by-second values of the speed time series with 30 km $h^{-1} < v < 40$ km h^{-1} and + 2.5 m^2 $s^{-3} < v\,a <$ + 7.5 m^2 s^{-3}.

Figure 1 Speed time series of Handbook real-world driving cycles R1, R2, R3 and R4. Each of the four driving cycles consists of three driving patterns, as indicated by the corresponding abbreviations. Cycle R1 is composed out of AE1, AE2 and A3 (all motorway driving); R2 consists of A4 (motorway), LE1 and LE2s (both rural driving); R3 is composed out of LE2u (rural driving), LE3 and LE5 (both urban driving); R4 consists of LE6 (urban driving), StGoHW and StGoUrb (motorway and urban stop-and-go driving, respectively)

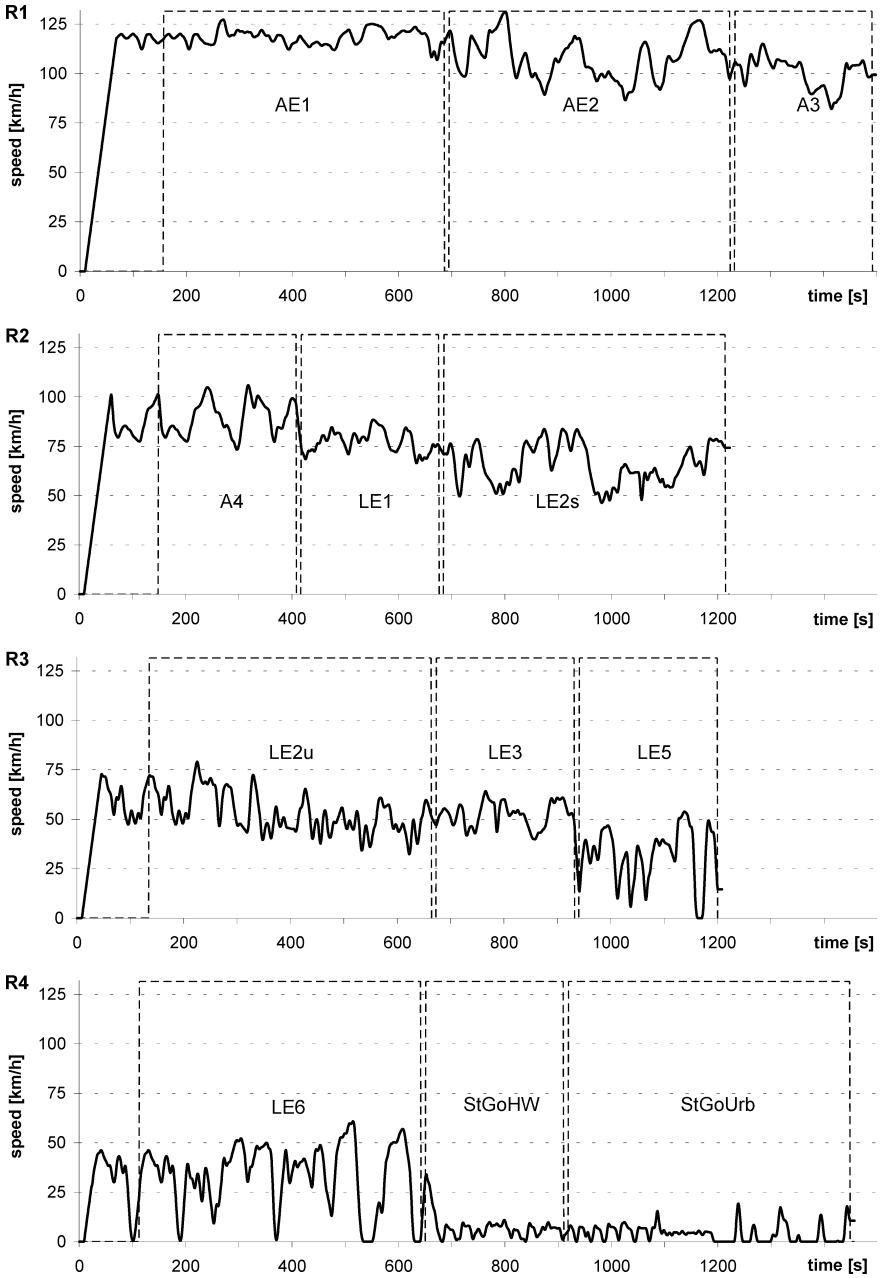

Figure 2 Kinematic representation [(v, v, a)-matrix] of driving patterns. Each second of the driving pattern is binned into a matrix according to the instantaneous speed and acceleration. The relative pattern of the resulting distribution is depicted. Horizontal axes are in $v \cdot a$ (speed multiplied with acceleration) in units $m^2\ s^{-3}$; vertical axes in v (speed) in units km h^{-1}

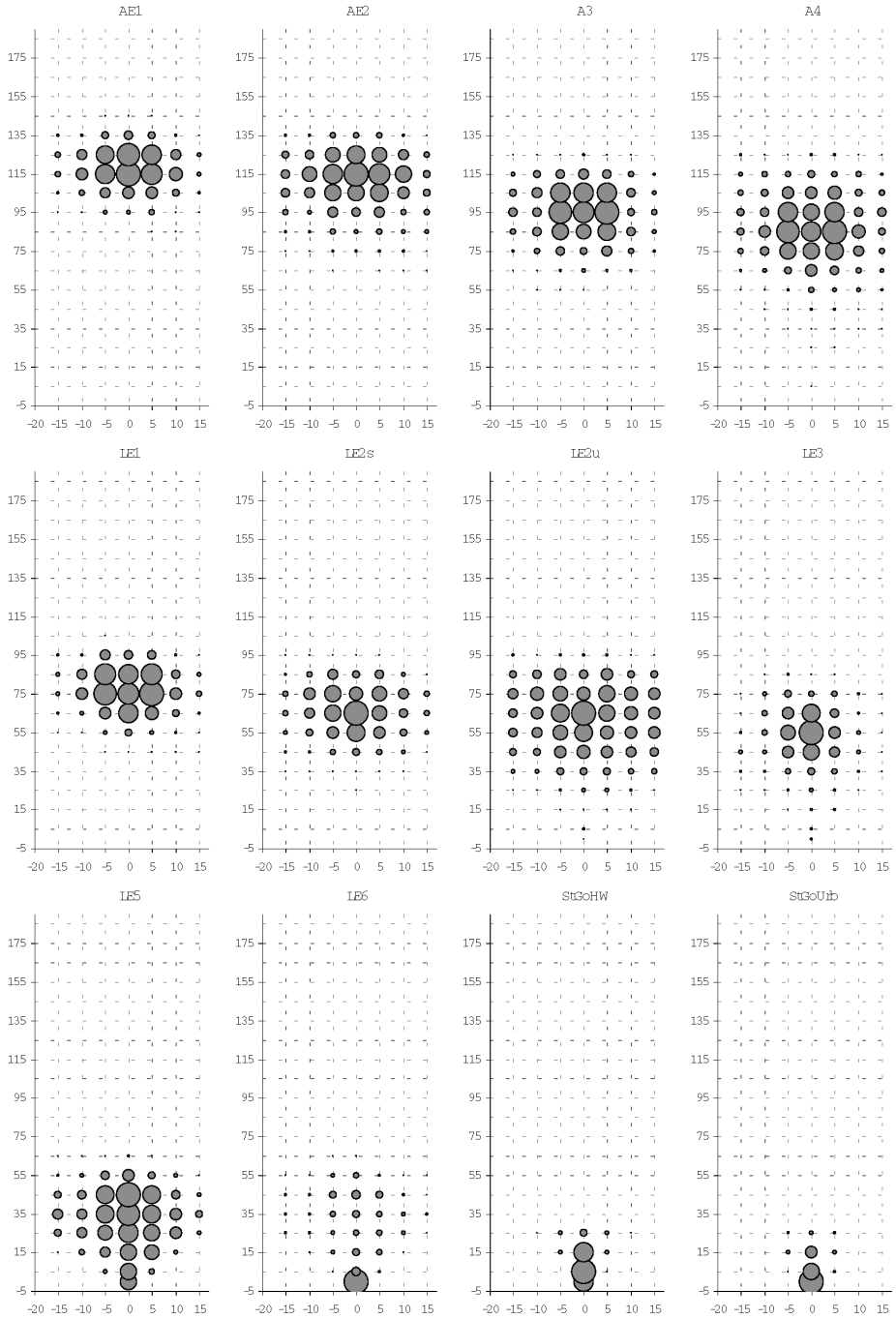

For the description of kinematic characteristics of the driving patterns, acceleration values (in ms^{-1}) for a speed profile consisting of n data rows of time in seconds, $t_i (1 \le i \le n)$, and speed in km/h, $v_i (1 \le i \le n)$, are computed as

$$a_i = \begin{cases} \dfrac{v_2 - v_1}{3.6(t_2 - t_1)} & (i = 1) \\ \dfrac{v_{i+1} - v_{i-1}}{3.6(t_{i+1} - t_{i-1})} & (2 \le i \le n-1) \\ \dfrac{v_n - v_{n-1}}{3.6(t_n - t_{n-1})} & (i = n) \end{cases} \tag{1}$$

Total stop time is then defined as

$$T_{\text{stop}} = \begin{cases} t_2 - t_1 & (v_1 = 0 \ \wedge \ a_1 = 0) \\ 0 & (\text{else}) \end{cases} + \sum_{i=2}^{n} \begin{cases} t_i - t_{i-1} & (v_i = 0 \ \wedge \ a_i = 0) \\ 0 & (\text{else}) \end{cases} \tag{2}$$

and total accelerating time as

$$T_{\text{acc}} = \begin{cases} t_2 - t_1 & (a_1 > a_L) \\ 0 & (\text{else}) \end{cases} + \sum_{i=2}^{n} \begin{cases} t_i - t_{i-1} & (a_i > a_L) \\ 0 & (\text{else}) \end{cases} \tag{3}$$

with $a_L = 0.06$ ms^{-2}. The average positive acceleration is

$$\overline{a}_{\text{pos}} = \left(\sum_{i=1}^{n} \begin{cases} 1 & (a_i > 0) \\ 0 & (\text{else}) \end{cases} \right)^{-1} \sum_{i=1}^{n} \begin{cases} a_i & (a_i > 0) \\ 0 & (\text{else}) \end{cases} \tag{4}$$

and the number of stops occurring during the driving pattern

$$\text{number of stops} = \sum_{i=1}^{n} \begin{cases} 1 & (\{v_i = 0 \ \wedge \ a_i = 0\} \ \wedge \{v_{i-1} \ne 0 \ \vee \ a_{i-1} \ne 0\}) \\ 0 & (\text{else}) \end{cases} \tag{5}$$

Relative positive acceleration (RPA) is defined as

$$\text{RPA} = \frac{1}{d} \sum_{i=1}^{n} \begin{cases} \dfrac{a_i v_i}{3.6} & (a_i > 0) \\ 0 & (\text{else}) \end{cases} \tag{6}$$

where d denotes the total driving distance of the driving pattern, $d = (t_2 - t_1) v_1 / 3.6 + \sum_{i=2}^{n} (t_i - t_{i-1}) v_i / 3.6$, and positive kinetic energy (PKE) is defined as

$$\text{PKE} = \frac{1}{d} \sum_{i=2}^{n} \begin{cases} v_i^2 - v_{i-1}^2 & (v_i > v_{i-1}) \\ & (\text{else}) \end{cases} \tag{7}$$

The resulting kinematic characteristics of the driving patterns are listed in Table 2, using the above equations. To visualise the dynamic content of the driving patterns, Figure 3 depicts RPA (equation (6)) and the standard deviation of positive acceleration (equation (4)) as a function of average speed, where average speed is d divided by total duration of the driving pattern (i.e., including stop time). As can be seen from Figure 3, there is a good correlation between these two parameters. The same holds for PKE (not shown).

Table 2 Kinematic characteristics of driving patterns

Full name	*Unit*	*AE1*	*AE2*	*A3*	*A4*	*LE1*	*LE2s*	*LE2u*	*LE3*	*LE5*	*LE6*	*StGoHW*	*StGoUrb*
Total distance	m	17417	15849	7247	6466	5575	9657	7792	3780	2307	4937	512	608
Total time	s	530	530	260	260	260	530	530	260	260	530	260	530
Percentage of cruising (%)	–	47.0	23.4	34.6	18.9	29.2	21.5	16.6	24.6	12.3	15.7	32.7	30.4
Percentage of time accelerating (%)	–	25.1	36.4	30.0	36.2	33.5	37.0	38.7	38.1	43.5	43.4	24.6	22.6
Percentage of time decelerating (%)	–	27.9	40.2	35.4	45.0	37.3	41.5	44.7	37.3	41.9	37.6	42.7	27.2
Percentage of time standing (stop time) (%)	–	0.0	0.0	0.0	0.0	0.0	0.0	0.0	0.0	2.3	3.4	0.0	19.8
Average speed (incl. stops)	km/h	118.3	107.6	100.3	89.5	77.2	65.6	52.9	52.3	31.9	33.6	7.1	4.1
Average pos. acc.	m/s^2	0.089	0.179	0.142	0.231	0.155	0.219	0.329	0.183	0.463	0.337	0.139	0.202
Standard dev. of acceleration	m/s^2	0.125	0.243	0.203	0.271	0.184	0.287	0.397	0.255	0.626	0.521	0.192	0.242
Standard dev. of pos. acc.	m/s^2	0.089	0.156	0.164	0.161	0.115	0.200	0.254	0.163	0.403	0.319	0.136	0.234
Number of accelerations	–	126	72	28	134	85	52	161	97	63	186	106	86
No. of acc. per km	1/km	7.2	4.5	3.9	20.7	15.2	5.4	20.7	25.7	27.3	37.7	207.1	141.4
Number of stops	–	0	0	0	0	0	0	0	0	1	2	0	7
Relative positive acceleration	m/s^2	0.044	0.086	0.070	0.101	0.072	0.108	0.147	0.092	0.194	0.164	0.041	0.113
Positive kinetic energy	m/s^2	1.140	2.236	1.823	2.620	1.895	2.817	3.862	2.405	5.033	4.249	1.079	2.957

Figure 3 Kinematic characteristics of the 12 driving patterns. Upper panel: relative positive acceleration (definition: equation (6)) as a function of average speed (computed over total cycle duration including stops). Lower panel: standard deviation of positive acceleration (definition: equation (4)) as a function of average speed.

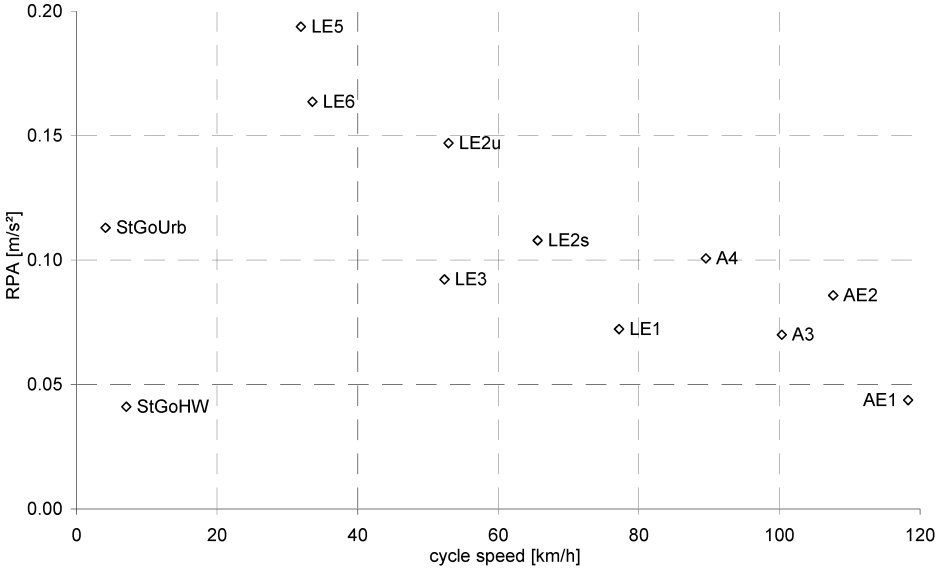

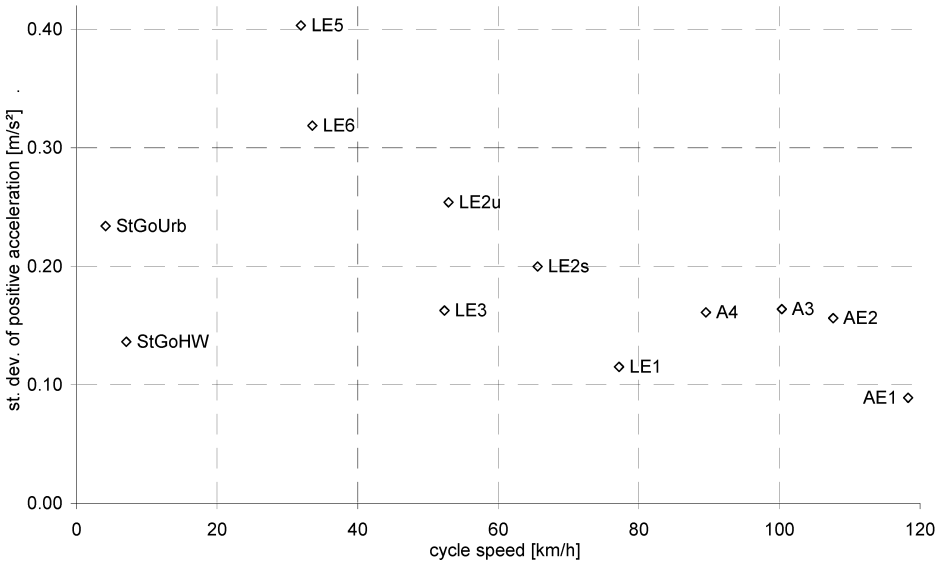

4 Illustrative example

The following example illustrates the principle of the proposed emission modelling method:

- As 'source' (cf. Section 2), the 12 driving patterns from HBEFA real-world driving cycles R1 to R4 are available (cf. Section 3), i.e., AE1, AE2, A3, A4, StGoHW (motorway driving), LE1, LE2s, LE2u, LE3, (rural), and LE5, LE6, StGoUrb (urban).
- As kinematic parameter, the (v, $v \cdot a$)-matrix is adopted (see Figure 2).
- Emissions are to be forecasted for four 'target' driving patterns for which no testbench measurements of driving patterns exist that are directly representative: D10, D7, D4, and D1. These are four out of a set of ten driving patterns describing urban and rural (but not motorway) driving behaviour in Germany within the HBEFA framework; they are used here for illustrative purposes only.
- For these driving patterns, representative speed time series do exist, from which the corresponding (v, $v \cdot a$)-matrices are computed. These are shown in Figure 4, uppermost row.
- Using a computer application, the optimal linear combinations of 'source' driving patterns is determined such that the sum of squared differences of the kinematic parameters, i.e., of the individual cells of the (v, $v \cdot a$)-matrices, become minimal. The (v, $v \cdot a$)-matrices of the linear combinations are shown in Figure 4 (centre row). The bottom row in Figure 4 depicts the squared differences for each of the matrix cells.
- The following constraints apply: the linear combination must not consist of more than three 'source' driving patterns; and the minimum increment in weights of the linear combination is 1%. These constraints have been arbitrarily set by the authors. Allowing for linear combinations with more than three driving patterns would reduce clarity of the approach and would enhance the risk that we adapt the model to effects caused by individual vehicles rather then systematical emission behavioural trends.

The resulting linear combinations are listed in Table 3. For driving patterns D1, D7 and D10, the allowed maximum of three driving patterns is being used, whereas a linear combination of only two driving patterns is optimal for D4 (i.e., this combination yields the minimal sum of squared differences over all cells of the (v, $v{\cdot}a$)-matrix). In all four cases, numerical values for both average speed and the average of speed times acceleration are identical (three relevant digits) for the driving pattern to be forecasted and for the linear combination used as forecast.

Figure 4 Illustrative example of emission factor modelling method. Uppermost row shows the kinematic representation [(v, v . a)-matrix, see caption to Figure 2] of the driving patterns whose emissions are to be forecasted. Centre row shows (v, v . a)-matrix of the linear combination of measured driving patterns, as listed in Table 3. The lowest row depicts the squared differences between cell shares of uppermost and centre row. From left to right, columns are for driving patterns D1, D4, D7 and D10, respectively

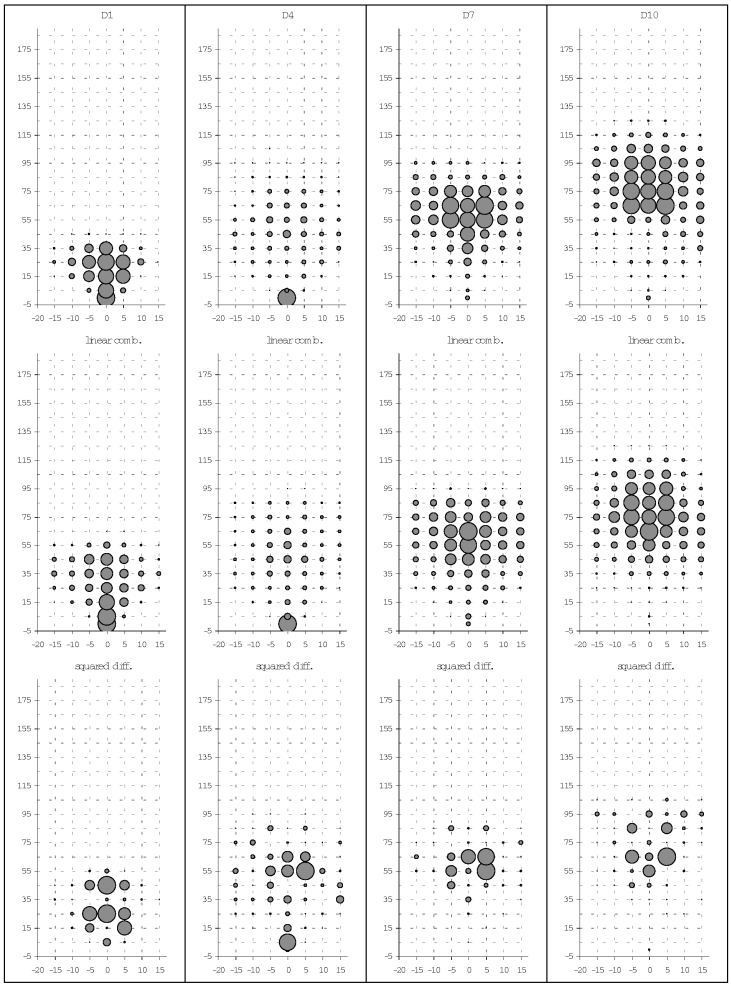

Table 3 Emission forecast for four driving patterns that have not been measured: optimal linear combinations of up to 3 out of the 12 measured driving patterns from real-world driving cycles R1–R4

Driving pattern	*Forecasted using linear combination of measured driving patterns*											
	AE1	*AE2*	*A3*	*A4*	*LE1*	*LE2s*	*LE2u*	*LE3*	*LE5*	*LE6*	*StGoHW*	*StGoUrb*
D1									72%		18%	10%
D4							38%			62%		
D7							77%	12%	11%			
D10			27%		27%		46%					

5 Measurements

Measurements conducted at EMPA are available for a total of 44 vehicles, which split up into three vehicle groups: 19 vehicles are gasoline passenger cars conforming to Euro-2 emission standards, 17 are gasoline passenger cars conforming to Euro-3, and eight are diesel passenger cars conforming to Euro-2. Individual vehicle data is listed in Table 4. More details on the experimental campaign can be found in (Stettler et al., 2004).

Table 4 Vehicle data

Unique identifier	*Vehicle make*	*Vehicle model*	*EURO legislation*	*Empty weight kg*	*Engine cap. ccm*	*Odometer km*	*First reg. year*	*Gear box type*	*Number of speeds*
passenger car EURO-2 gasoline									
EMPA_PCG052	VW	Polo	EURO-2	955	1400	40,464	1997	manual	5
EMPA_PCG053	Renault	Twingo	EURO-2	835	1195	59,800	1997	manual	5
EMPA_PCG054	Ford	Ka 1.3	EURO-2	908	1265	47,530	1997	manual	5
EMPA_PCG056	Fiat	Punto 55	EURO-2	865	1315	61,896	1997	manual	5
EMPA_PCG057	Kia	Pride 1.3	EURO-2	793	1260	53,400	1997	manual	5
EMPA_PCG058	Skoda	Felicia 1.3	EURO-2	960	1420	53,470	1997	manual	5
EMPA_PCG059	Opel	Vectra B20 Caravan	EURO-2	1375	1940	104,700	1997	manual	5
EMPA_PCG060	Audi	A3	EURO-2	1200	1655	62,835	1997	manual	5
EMPA_PCG061	Toyota	Corolla 1600	EURO-2	1116	1650	62,616	1998	manual	5
EMPA_PCG062	Mercedes-Benz	A160	EURO-2	1045	1500	34,168	1998	manual	5
EMPA_PCG064	Hyundai	Lantra 2.0	EURO-2	1235	1715	48,240	1997	manual	5
EMPA_PCG065	Peugeot	306 Break 1.6	EURO-2	1175	1605	89,523	1998	manual	5
EMPA_PCG066	Ford	Mondeo 2.0	EURO-2	1335	1840	57,920	1997	manual	5
EMPA_PCG067	Mitsubishi	Carisma 1.8 GDI	EURO-2	1235	1685	59,100	1997	manual	5
EMPA_PCG068	Peugeot	406 2.0 T Break 5	EURO-2	1461	1998	58,100	1997	manual	5
EMPA_PCG069	Subaru	Impreza 2.0 4WD	EURO-2	1235	1680	52,000	1997	autom	4
EMPA_PCG070	BMW	Z3	EURO-2	1160	1410	78,200	1997	manual	5
EMPA_PCG072	Fiat	Ulysse 2.0	EURO-2	1546	2300	61,604	1997	manual	5
EMPA_PCG078	Porsche	Boxster	EURO-2	1310	1610	22,200	1997	autom.	5
Average				1144	1602	58,303	1997.2		

Table 4 Vehicle data (continued)

	Unique identifier	*Vehicle make*	*Vehicle model*	*EURO legislation*	*Empty weight kg*	*Engine cap. ccm*	*Odometer km*	*First reg. year*	*Gear box type*	*Number of speeds*
Passenger car EURO-3 gasoline	EMPA_PB3-01	Toyota	Yaris 1.0	EURO-3	900	1320	37,306	2000	manual	5
	EMPA_PB3-02	MCC	Smart	EURO-3	720	980	19,482	2000	autom.	6
	EMPA_PB3-03	Citroen	Xsara1.4i	EURO-3	1116	1666	21,093	2001	manual	5
	EMPA_PB3-04	Hyundai	Accent1.3 GS	EURO-3	990	1555	22,300	2000	manual	5
	EMPA_PB3-05	Mazda	Demio	EURO-3	1025	1475	20,465	2001	manual	5
	EMPA_PB3-06	Ford	Focus 1.6 16V	EURO-3	1151	1620	19,020	2000	autom.	4
	EMPA_PB3-07	Renault	Megane 1.6 16V	EURO-3	1120	1600	20,300	2001	manual	5
	EMPA_PB3-08	Fiat	Punto 1.8HGT	EURO-3	1020	1550	21,500	2000	manual	5
	EMPA_PB3-09	Peugeot	306 1.8 16V	EURO-3	1170	1600	18,700	2001	manual	5
	EMPA_PB3-10	Opel	Zafira 1.8 16V	EURO-3	1390	2010	34,000	2000	autom.	4
	EMPA_PB3-11	AlfaRomeo	147 2.0 TS 16V	EURO-3	1303	1790	30,000	2001	manual	5
	EMPA_PB3-12	Honda	Accord 2.0i VTEC	EURO-3	1425	1930	28,300	2000	manual	5
	EMPA_PB3-13	Renault	Megane Scenic 2.0	EURO-3	1325	1815	80,400	2001	manual	5
	EMPA_PB3-14	Nissan	Primera 2.0 CVT	EURO-3	1325	1780	29,985	2000	autom.	0
	EMPA_PB3-15	Ford	Mondeo 2.0	EURO-3	1385	2030	31,200	2001	manual	5
	EMPA_PB3-17	BMW	323 Ci	EURO-3	1370	1870	28,460	2000	manual	5
	EMPA_PB3-18	Mitsubishi	Galant 2.5 V6	EURO-3	1445	1835	33,086	2000	autom.	5
	Average				1187	1672	29,153	2000.4		
Pass car EURO-2 diesel	EMPA_PD2-01	Ford	Focus 1.8 TD	EURO-2	1273	1755	35,800	2000	manual	5
	EMPA_PD2-02	Seat	Ibiza GT TDI	EURO-2	1105	1565	31,150	1999	manual	5
	EMPA_PD2-03	VW	Passat	EURO-2	1375	1850	103,320	2001	manual	5
	EMPA_PD2-04	Peugeot	406 1.9 DT	EURO-2	1365	1832	93,600	1997	manual	5
	EMPA_PD2-05	Opel	Zafira A 20 TD	EURO-2	1430	2065	68,700	1999	manual	5
	EMPA_PD2-06	AlfaRomeo	156 2.4 JTD	EURO-2	1410	1850	70,980	1998	manual	5
	EMPA_PD2-07	Mercedes-Benz	C250 TD	EURO-2	1405	1960	62,614	1997	autom.	5
	EMPA_PD2-08	Mitsubishi	Pajero 2.8 TDI	EURO-2	1990	2720	59,300	1999	manual	5
	Average				1419	1950	65,683	1998.8		

For each vehicle, for all four driving cycles shown in Figure 1, measurements are available on the emissions of nitrogen oxides (NO_x, expressed in NO_2 mass equivalents), without humidity correction applied, carbon monoxide (CO), total content of hydrocarbons including methane (HC, expressed in $C_1H_{1.85}$ mass equivalents), mass of particulate matter (PMm) (for diesel vehicles only), and carbon dioxide (CO_2). Fuel consumption has been computed from the emissions of CO_2, HC, CO, and PMm. The resulting emissions per driving pattern, averaged per vehicle group, are listed in Table 5.

Table 5 Averaged emission factors from bag measurements

		Emission factor [g/km]					
	Driving pattern	*CO*	CO_2	*FC*	*HC*	NO_x	*PMm*
Passenger car EURO-2 gasoline	AE1	0.810	176.3	55.8	0.040	0.214	
	AE2	1.548	159.9	51.0	0.052	0.166	
	A3	0.837	148.0	46.9	0.040	0.127	
	A4	0.985	140.4	44.6	0.064	0.107	
	LE1	0.258	120.1	37.8	0.026	0.060	
	LE2s	0.464	124.9	39.4	0.027	0.077	
	LE2u	0.725	132.3	41.9	0.048	0.087	
	LE3	0.232	125.3	39.4	0.023	0.060	
	LE5	0.702	177.7	56.2	0.078	0.112	
	LE6	0.707	185.8	58.7	0.072	0.095	
	StGoHW	0.985	394.7	124.4	0.098	0.089	
	StGoUrb	2.573	625.7	197.9	0.305	0.143	
Passenger car EURO-3 gasoline	AE1	0.550	175.5	56.2	0.017	0.040	
	AE2	1.199	161.8	52.2	0.017	0.027	
	A3	0.891	147.6	47.5	0.015	0.020	
	A4	0.717	140.9	45.3	0.015	0.024	
	LE1	0.232	119.8	38.3	0.007	0.013	
	LE2s	0.242	122.1	39.1	0.004	0.018	
	LE2u	0.273	131.6	42.1	0.006	0.042	
	LE3	0.163	121.6	38.9	0.003	0.020	
	LE5	0.327	170.9	54.6	0.006	0.047	
	LE6	0.247	168.2	53.7	0.005	0.044	
	StGoHW	0.318	357.0	114.0	0.006	0.029	
	StGoUrb	1.312	537.3	171.9	0.081	0.029	
Passenger car EURO-2 diesel	AE1	0.070	183.8	58.6	0.026	0.769	0.061
	AE2	0.066	169.9	54.2	0.023	0.756	0.051
	A3	0.060	148.1	47.2	0.023	0.602	0.039
	A4	0.055	139.3	44.4	0.020	0.544	0.034
	LE1	0.061	118.9	37.9	0.021	0.426	0.031
	LE2s	0.127	117.2	37.4	0.028	0.476	0.034
	LE2u	0.162	124.5	39.8	0.033	0.542	0.038
	LE3	0.162	115.3	36.8	0.039	0.418	0.029
	LE5	0.344	163.7	52.3	0.084	0.668	0.050
	LE6	0.286	162.6	52.0	0.084	0.618	0.041
	StGoHW	0.955	319.4	102.3	0.260	1.471	0.073
	StGoUrb	1.614	477.3	152.9	0.421	2.553	0.119

6 Validation

In order to assess the robustness of the proposed methodology, a cross-validation has been performed. For each of the 12 driving patterns shown in Table 2, an emission forecast has been computed using the other 11 driving patterns as ‘source’ driving

patterns, but not the driving pattern to be forecasted itself. Hence the model had to be run 12 times, because each time there is a different set of available 'source' driving patterns.

The emission modelling method proposed in this paper may be regarded as being a sophisticated interpolation method. In the space constituted by the kinematic parameters that have been chosen for the modelling (in our illustrative example, the (v, $v{\cdot}a$)-matrix), a good emission prediction may therefore be expected for driving patterns that are situated among driving patterns (for which measurements are available). However, should a driving pattern be extreme (with respect to the kinematic parameters adopted) with regard to the available driving patterns, the method actually must extra- rather than interpolate. This will lead to a decrease in prediction power.

From an ex ante perspective, therefore, one would expect that for the present cross-validation, the driving patterns StGoUrb, StGoHW, LE5, LE3, and AE1 will be more difficult to predict, since they are extreme with respect to the other driving patterns (see Figure 3).

Table 6 shows the resulting linear combination for each of the 12 driving patterns. The relative errors of the resulting emission factors are depicted in Figure 5 for CO_2 (upper panel) and NO_x (lower panel). As can be seen, the model predicts best for those driving patterns that are not extreme with respect to the relevant kinematic parameters (i.e., the model operates within the interpolation area). Of all 12 driving patterns, severe problems occur for StGoUrb. This driving pattern apparently has unique characteristics, and cannot be predicted adequately even by StGoHW.

Overall, a good prediction capability is reached; the average of the absolute relative error is 8% for CO_2 and fuel consumption (FC), 20% for NO_x, 42% for CO, and 41% for HC. The bias, i.e., the average of the signed relative errors, is –3% for CO_2 and FC, 4% for NO_x, 17% for CO and 21% for HC. Prediction capability is most influenced by the prediction of the StGoUrb pattern. This pattern clearly is unique with respect to its emission behaviour, which is not covered by any of the other driving patterns. Therefore, the present method basically being an interpolation method, StGoUrb cannot be predicted with acceptable quality.

Table 6 Linear combinations used in the cross-validation; each of the 12 measured driving patterns is forecasted using the results from the other 11 driving patterns

Driving pattern:	*... is forecasted by the following linear combination*		
AE1	100% AE2		
AE2	3% LE5	26% A3	71% AE1
A3	21% AE2	79% A4	
A4	3% LE5	44% LE1	53% A3
LE1	64% LE2s	36% A4	
LE2s	22% LE1	23% LE3	55% LE2u
LE2u	12% A4	20% LE5	68% LE2s
LE3	20% LE1	40% LE2s	40% LE2u
LE5	88% LE6	10% LE2u	2% StGoUrb
LE6	37% LE3	54% LE5	9% StGoUrb
StGoHW	40% StGoUrb	60% LE5	
StGoUrb	85% StGoHW	15% LE6	

Figure 5 Relative prediction error when forecasting each of the 12 driving patterns using linear combinations of the measured bag data from the other 11 driving patterns (cross-validation). Upper panel: CO_2; lower panel: NO_x

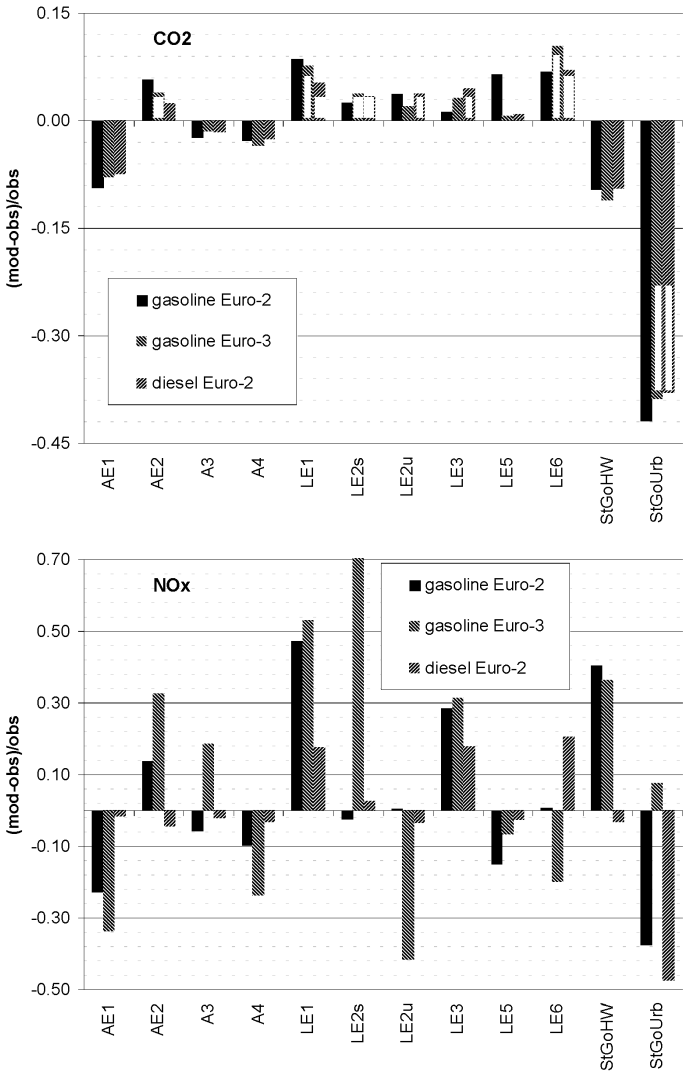

7 Discussion

For fleet emission modelling approaches, which do not rely upon vehicle-specific information, instantaneous modelling will become less powerful as vehicles become more complex and more individualistic. The use of testbench results from real-world driving cycles can be used as alternative. The design and testing of these real-world test cycles is of prime importance. The more representative, the better the emission prediction will be. The test cycles should be split up into driving patterns that are diverse among each other and homogeneous themselves. Emission modelling in this context merely is an

interpolating method, telling the user which weighted set of driving patterns, for which emission measurements are available, is the best approximation for the driving pattern whose emissions are to be predicted.

The present paper presents a method for this interpolation procedure. It is flexible in the sense that the user may select which kinematic parameter is best suited to explain the variability of emission behaviour among the different driving patterns. It determines the linear combination of driving patterns that is mathematically optimal by minimising the sum of squared differences between target (driving pattern) and model (linear combination).

Acknowledgements

The present work has been funded by the Swiss Agency for Environment, Forests and Landscape (SAEFL).

References

Chang, T-J. (2002) 'Numerical evaluation of the effect of traffic pollution on indoor air quality of a naturally ventilated building', *Journal of the Air & Waste Management Association*, Vol. 52, No. 9, pp.1043–1053.

Dab, W., Ségala, W., Dor, F., Festy, B., Lameloise, P., Le Moullec, Y., Le Tertre, A., Médina, S., Quénel, P., Wallaert, B. and Zmirou, D. (2001) 'Air pollution and health: correlation or causality? The case of the relationship between exposure to particles and cardiopulmonary mortality', *Journal of the Air & Waste Management Association*, Vol. 2001, No. 2, pp.220–235.

de Haan, P. and Keller, M. (2000) 'Emission factors for passenger cars: application of instantaneous emission modeling', *Atmospheric Environment*, Vol. 34, pp.4629–4638.

de Haan, P. and Keller, M. (2001) *Real-world Driving Cycles for Emission Measurements: ARTEMIS and Swiss Cycles*, in *Folgearbeiten SRU 255 Nachtrag Arbeitsunterlage 25*, under a contract to Swiss Agency for Environment, Forests and Landscape (SAEFL), to be obtained from SAEFL, 3003 Bern, Switzerland.

de Haan, P., Rotach, M.W. and Werfeli, M. (2001) 'Modification of an operational dispersion model for urban applications', *Journal Applied Meteorology*, Vol. 40, pp.864–879.

Fischer, P.H., Hoek, G., van Reeuwijk, H., Briggs, D.J., Lebret, E., van Wijnen, J., Kingham, S. and Elliott, P.E. (2000) 'Traffic-related differences in outdoor and indoor concentrations of particles and volatile organic compounds in Amsterdam', *Atmospheric Environment*, Vol. 34, pp.3713–3722.

Hoek, G., Brunekreef, B., Verhoeff, A., van Wijnen, J. and Fischer, P. (2000) 'Daily mortality and air pollution in the Netherlands', *Journal of the Air & Waste Management Association*, Vol. 50, No. 8, pp.1380–1389.

INFRAS (1995) *Handbook Emission Factors from Road Transport (HBEFA) 1.2, CD-ROM*, under a contract to Swiss Agency for the Environment, Forests and Landscape (SAEFL) and Federal Environmental Protection Agency Germany (UBA Berlin).

Janssen, N.A.H., van Vliet, P.H.N., Aarts, F., Harssema, H. and Brunekreef, B. (2001) 'Assessment of exposure to traffic related air pollution of children attending schools near motorways', *Atmospheric Environment*, Vol. 35, No. 22, pp.3875–3884.

Keller, M. and de Haan, P. (1999) *Luftschadstoffemissionen des Strassenverkehrs 1950–2020. Nachtrag*, in *Schriftenreihe Umwelt (SRU) 255 Nachtrag*, Swiss Agency for Environment Forests and Landscape (SAEFL).

Keller, M., Kessler, H. and Heldstab, J. (1995) *Luftschadstoff-Emissionen des Strassenverkehrs 1950–2010 (in German, with English abstract)*, in *Schriftenreihe Umwelt 255*. Swiss Agency for Environment, Forests and Landscape (SAEFL), to be obtained from SAEFL, 3003 Bern, Switzerland.

Kunzli, N., Kaiser, R., Medina, S., Studnicka, M., Chanel, O., Filliger, P., Herry, M., Horak Jr., F., Puybonnieux-Texier, V., Quénel, P., Schneider, J., Seethaler, R., Vergnaud, J-C. and Sommer, H. (2000) 'Public-health impact of outdoor and traffic-related air pollution: a European assessment', *Lancet*, Vol. 356, pp.795–801.

Ntziachristos, L. and Samaras, Z. (2000) 'Speed dependent representative emission factors for catalyst passenger cars and influencing parameters', *Atmospheric Environment*, Vol. 34, No. 27, pp.4611–4619.

Pope, C.A., Dockery, D.W. and Schwartz, J. (1995) 'Review of epidemiological evidence of health effects of particulate air pollution', *Inhalation Toxicology*, Vol. 7, pp.1–18.

Sapkota, A. and Buckley, T.J. (2003) 'The mobile source effect on curbside 1,3-butadiene, benzene, and particle-bound polycyclic aromatic hydrocarbons assessed at a tollbooth', *Journal of the Air & Waste Management Association*, Vol. 53, No. 6, pp.740–748.

Skov, H., Hansen, A.B., Loreznzen, G., Vibeke Andersen, H., Löfström, P. and Christensen, C.S. (2001) 'Benzene exposure and the effect of traffic pollution in Copenhagen, Denmark', *Atmospheric Environment*, Vol. 35, pp.2463–2471.

Stahel, W., Pritscher, L., de Haan, P. and Keller, M. (2000) *Neues EMPA-Standardmessprogramm (in German)*, in *Folgearbeiten SRU 255 Nachtrag, Arbeitsunterlage 19*, under a contract to Swiss Agency for Environment, Forests and Landscape (SAEFL), to be obtained from SAEFL, 3003 Bern, Switzerland.

Stettler, P., Weilenmann, M. and Heeb, N. (2004) *Nachführungen der Emissionsgrundlagen Strassenverkehr, Ergänzungen der Messdaten: Personenwagen-Messungen 2001–2002*, in *EMPA Research Report 202114*.

Sturm, P.J., Hausberger, S., Keller, M. and de Haan, P. (2000) 'Estimating real-world emissions from passenger cars – use and limitations of instantaneous emissions data', *International Journal Vehicle Design*, Vol. 24, pp.19–33.

Vardoulakis, S., Gonzalez-Flesca, N. and Fisher, B.E.A. (2002) 'Assessment of traffic-related air pollution in two street canyons in Paris: implications for exposure studies', *Atmospheric Environment*, Vol. 36, No. 6, pp.1025–1039.